

Window function dependence of the novel mass function of primordial black holes

Koki Tokeshi,^{a,b} Keisuke Inomata,^b and Jun'ichi Yokoyama^{a,b,c}

^aDepartment of Physics, Graduate School of Science, The University of Tokyo,
7-3-1 Hongo, Bunkyo, Tokyo, 113-0033, Japan

^bResearch Center for the Early Universe (RESCEU), Graduate School of Science,
The University of Tokyo, 7-3-1 Hongo, Bunkyo, Tokyo, 113-0033, Japan

^cKavli Institute for the Physics and Mathematics of the Universe (Kavli IPMU),
The University of Tokyo, 5-1-5 Kashiwanoha, Kashiwa, Chiba, 277-8583, Japan

E-mail: tokeshi@resceu.s.u-tokyo.ac.jp, inomata@resceu.s.u-tokyo.ac.jp,
yokoyama@resceu.s.u-tokyo.ac.jp

Abstract. We investigate the ambiguity of the novel mass function of primordial black holes, which has succeeded in identifying the black hole mass in a given configuration of fluctuations, due to the choice of window function of smoothed density fluctuations. We find that while the window function dependence of the exponential factor in the novel mass function is the same as the one in the conventional mass function around the top-hat scale, the dependences are different on other scales, which leads to the narrower mass function in the novel formulation for some window functions.

Keywords: primordial black hole, window function

ArXiv ePrint: [XXXX.XXXX](#)

Contents

1	Introduction	1
2	Basic formulas for PBH formation	2
3	Review on window functions and their properties	5
4	Window function dependence of the novel mass function	7
5	Conclusion and discussion	10
A	The novel mass function in the 4-dimensional spacetime	12

1 Introduction

Primordial black holes (PBHs) are produced in the early Universe when the density fluctuations larger than the threshold enter the Hubble horizon [1–3]. The formation of PBHs and its cosmological implications have been discussed from a variety of viewpoints for several decades [4–8]. PBHs are candidates for a portion of the dark matter (DM) and some heavy BHs recently observed by the LIGO-Virgo collaboration [9–19]. In addition, the abundance of PBHs can give us some clues of small-scale density fluctuations that are related to properties of inflation models but not accessible by cosmic microwave background (CMB) or the large-scale structure observations [20–27]. (See also refs. [28, 29] for recent reviews on PBHs.)

The relation between the power spectrum of curvature perturbations, related to the inflation models, and the PBH mass function has been studied in refs. [30–35] with the use of the Press–Schechter formalism [36] or the peaks theory [37]. However, as pointed out in ref. [38], the mass functions so far have some issues at the conceptual level, which stem from the fact that the conventional PBH formation criteria are not enough for straightforwardly giving the mass function, defined as a differential quantity. Recently the authors in ref. [38] have deduced that a PBH is produced around a certain peak at the mass scale where smoothed density perturbation around it takes the maximum value as the smoothing scale R and corresponding mass scale are changed. From this observation they have proposed a new additional criterion for PBH formation to avoid the issues, which is to require the smoothed density fluctuation to be maximal with the change of R . With this additional criterion, they have succeeded in defining a novel mass function. Also, the same criterion is proposed in ref. [39]. Although the prefactor of the mass function in ref. [39] is different from the one in ref. [38], which comes from the difference of other imposed conditions, the exponential factors in both mass functions are similar to each other.

Since PBH formation is a phenomenon occurring on the horizon scale at the formation time, we expect that the PBH formation should not depend on the perturbations on the deeply subhorizon. In other words, we expect that the contribution of the subhorizon perturbations to the PBH formation must be suppressed. To take into account this suppression, the window (or filter/smoothing) function has been introduced in many references.¹

¹ In ref. [33], the authors do not use the window function and, instead relate a PBH mass with the height and the curvature of the peak. However, the analysis cannot be applied to broad or multiple-peak power spectra of curvature perturbations [33].

However, there is no consensus on the choice of the window function so far. The window function dependence of the conventional mass function has been studied on in refs. [40, 41], which focus on the window function dependences of the smoothed density contrast [40, 41] and the threshold [41]. However, unlike the conventional mass function, the novel mass function includes in its exponential factor the density contrasts differentiated with respect to the smoothing scale, as we will see in section 2. Since the mass function sensitively depends on its exponential factor, it is worthwhile to revisit the window function dependence of the factor. In this paper, we discuss the window function dependence, specifically taking the following three window functions, which are used in the literature, namely, the Gaussian window function and the top-hat window functions in position space and wavenumber space which we call x -space top-hat and k -space top-hat window functions, respectively. Then, we report the updated window function dependence of the exponential factor.

The rest of the paper is organized as follows. In section 2, we review the basic formulas needed to carry out our discussion. Then, we review the three kinds of window functions and the behavior of the smoothed density contrast in section 3. In section 4, we discuss the window function dependence of the novel mass function. Finally, we devote section 5 to conclusion and discussion.

2 Basic formulas for PBH formation

In this section, we briefly summarize the basic formulas for PBH formation, which are mainly based on the formulation recently reported in ref. [38]. Note that we assume that PBHs are produced during the radiation-dominated era throughout this paper.

Density contrast One of the useful quantities to describe PBH formation is the density contrast on the comoving slice, which is defined as $\delta \equiv \delta\rho/\bar{\rho}$ with $\bar{\rho}$ and $\delta\rho$ being the background and the perturbation of the energy density, respectively. We can express the density contrast in terms of the curvature perturbation \mathcal{R} at linear order as²

$$\delta(\mathbf{x}) \simeq -\frac{4}{9} \frac{1}{(aH)^2} \nabla^2 \mathcal{R}(\mathbf{x}) , \quad (2.1)$$

where this relation is valid on superhorizon scales and in the radiation-dominated era. Here, $1/(aH)$ denotes the conformal Hubble horizon with a and H being the scale factor and the Hubble parameter, respectively. Since the PBH formation is expected not to be affected by modes deep inside the horizon, it should be described by the density contrast that is coarse-grained through some window function $W(R, r)$ with the smoothing scale R being the horizon scale $1/(aH)$ as

$$\begin{aligned} \delta(R, \mathbf{x}) &\equiv \int d^3y W(R, |\mathbf{y} - \mathbf{x}|) \delta(\mathbf{y}) \\ &\simeq -\frac{4}{9} R^2 \int d^3y W(R, |\mathbf{y} - \mathbf{x}|) \nabla^2 \mathcal{R}(\mathbf{y}) . \end{aligned} \quad (2.2)$$

Hereafter, we call $\delta(R, \mathbf{x})$ the smoothed density contrast and denote it by $\delta_R(\mathbf{x})$ or δ_R for short. The concrete expressions of the window functions will be given in section 3.

²The effects of the non-linear relation between δ and \mathcal{R} on the PBH abundance have been discussed in refs. [42–45].

Power spectrum of curvature perturbation The power spectrum of the curvature perturbation is defined with their Fourier modes, $\tilde{\mathcal{R}}$, as

$$\langle \tilde{\mathcal{R}}(\mathbf{k})\tilde{\mathcal{R}}(\mathbf{k}') \rangle = (2\pi)^3 \delta_{\text{D}}(\mathbf{k} + \mathbf{k}') \frac{2\pi^2}{k^3} \mathcal{P}_{\mathcal{R}}(k), \quad (2.3)$$

where the angle brackets stand for the ensemble average, $\delta_{\text{D}}(x)$ is the Dirac δ -function, and $k = |\mathbf{k}|$. To make the discussion concrete, we take the top-hat power spectrum as a fiducial example throughout this paper, given by

$$\mathcal{P}_{\mathcal{R}}(k) = \mathcal{A}\Theta(k - k_l)\Theta(-k + k_s), \quad (2.4)$$

where \mathcal{A} is the amplitude of the power spectrum, $\Theta(x)$ is the Heaviside step function, and both k_l and k_s are the cut-off wavenumbers ($0 < k_l < k_s$).³

PBH mass function Here, we review the novel PBH mass function recently reported in ref. [38], which imposes the following criteria for PBH formation:

$$\delta(R, \mathbf{x}) > \delta_{\text{th}}, \quad \frac{\partial \delta(R, \mathbf{x})}{\partial x^\alpha} = 0, \quad \lambda_\alpha(H) < 0, \quad (2.5)$$

where x^α runs over the 3-dimensional space coordinates and R , that is, x^i with $i = 1, 2, 3$ denote the space coordinates and x^4 denotes the smoothing scale R . λ_α 's are the eigenvalues of the 4×4 Hesse matrix for $\delta(R, \mathbf{x})$, that is, $H_{\alpha\beta} = \partial^2 \delta(R, \mathbf{x}) / \partial x^\alpha \partial x^\beta$. The first condition requires that PBH formation occurs if the smoothed density contrast exceeds some threshold δ_{th} . The second and the third conditions guarantee that, at the point of formation, $\delta(R, \mathbf{x})$ becomes not only extremum but also maximum with respect to the 4-dimensional parameter space x^α . The novel point of this formulation is adding the smoothing scale R to the coordinates and imposing the same condition even for R so that each high density peak, which would eventually collapse to a PBH, would be counted as such at the proper mass scale. The three conditions in eq. (2.5) lead to the novel expression of the mass function with PBH mass M [38],

$$f(M) = \frac{M}{n_{\text{PBH}}} \int dR \left\langle |\det H| \delta_{\text{D}}(M - m(R, \delta_R)) \Theta(\delta_R - \delta_{\text{th}}) \prod_{\alpha=1}^4 \delta_{\text{D}}(\delta_{R,\alpha}) \Theta(-\lambda_\alpha) \right\rangle, \quad (2.6)$$

where $f(M)$ denotes the relative fraction of PBHs within unit logarithmic mass interval around M , which satisfies $\int d \ln M f(M) = 1$. The variables after commas represent derivatives with respect to them and m and n_{PBH} are the mass of a PBH related to each peak and the comoving number density of PBHs, respectively. Here, we neglect the effects of the critical phenomena [46–49] and assume that the PBH mass depends only on the smoothing scale for the sake of comparison with conventional approach. Then, we can rewrite eq. (2.6) as

$$f(M) = \frac{M}{n_{\text{PBH}} \partial m(R) / \partial R} I(M), \quad (2.7)$$

³Throughout this paper, we just assume that the value of $\Theta(0)$ is finite, that is, do not assume any specific value of $\Theta(0)$, though it appears in Eqs. (4.5) and (4.6). This is because the final result of the exponential factor does not depend on the finite value of $\Theta(0)$ due to the divergent factors in Eqs. (4.5) and (4.6).

where

$$I(M) \equiv \left\langle |\det H| \Theta(\delta_R - \delta_{\text{th}}) \prod_{\alpha=1}^4 \delta_{\text{D}}(\delta_{R,\alpha}) \Theta(-\lambda_\alpha) \right\rangle. \quad (2.8)$$

In the case where the probability distribution of δ_R is Gaussian,⁴ the analytical expression of eq. (2.8) can be obtained by rewriting the Heaviside step function and the Dirac δ -functions in terms of the inverse Fourier transformations. Doing so, we finally obtain

$$\begin{aligned} I(M) = & \frac{1}{\sqrt{\det(2\pi L)}} \sqrt{\frac{2}{N_{55}}} \\ & \times \left[\left(A + B_{ij} N_{ij} + 3C_{ijkl} N_{ij} N_{kl} - \frac{(B_{ij} + 6C_{ijkl} N_{kl}) N_{i5} N_{j5}}{N_{55}} + \frac{3C_{ijkl} N_{i5} N_{j5} N_{k5} N_{l5}}{N_{55}^2} \right) \right. \\ & \times \frac{\sqrt{\pi}}{2} \text{erfc} \left(\sqrt{\frac{N_{55}}{2}} \delta_{\text{th}} \right) \\ & + \frac{\delta_{\text{th}}}{\sqrt{2N_{55}}} \left((B_{ij} + 6C_{ijkl} N_{kl}) N_{i5} N_{j5} + \frac{\delta_{\text{th}} (3 + N_{55} \delta_{\text{th}}^2) C_{ijkl} N_{i5} N_{j5} N_{k5} N_{l5}}{N_{55}} \right) \\ & \left. \times \exp \left(-\frac{N_{55}}{2} \delta_{\text{th}}^2 \right) \right], \quad (2.9) \end{aligned}$$

where L is the symmetric and block diagonal 5×5 matrix defined by

$$L \equiv \begin{pmatrix} \langle (\delta_{R,x})^2 \rangle & & & & \\ & \langle (\delta_{R,y})^2 \rangle & & & \\ & & \langle (\delta_{R,z})^2 \rangle & & \\ & & & \langle (\delta_{R,R})^2 \rangle & \langle \delta_{R,R} \delta_R \rangle \\ & & & \langle \delta_{R,R} \delta_R \rangle & \langle \delta_R^2 \rangle \end{pmatrix}, \quad (2.10)$$

and N is the inverse matrix of L . See appendix A for the derivation of eq. (2.9) and the explicit expressions for N and the other quantities, such as A , B_{ij} , and C_{ijkl} . In the rest of this paper, we focus on the exponential factor in eq. (2.9), given by

$$\frac{N_{55}}{2} \delta_{\text{th}}^2 = \frac{1}{2} N_{55} \langle \delta_R^2 \rangle \frac{\delta_{\text{th}}^2}{\langle \delta_R^2 \rangle} = \frac{1}{2} \frac{\langle \delta_R^2 \rangle \langle (\delta_{R,R})^2 \rangle}{\langle \delta_R^2 \rangle \langle (\delta_{R,R})^2 \rangle - \langle \delta_R \delta_{R,R} \rangle^2} \frac{\delta_{\text{th}}^2}{\langle \delta_R^2 \rangle}. \quad (2.11)$$

The abundance of PBHs strongly depends on this exponential factor. Note that eq. (2.11) has the same form as the 2-dimensional toy model result obtained in ref. [38]. Comparing eq. (2.11) with the corresponding exponential factor of the conventional mass function, $(1/2) \delta_{\text{th}}^2 / \langle \delta_R^2 \rangle$ [31], we observe that the extra factor $N_{55} \langle \delta_R^2 \rangle$ is additionally multiplied in the novel formulation. In other words, the deviation of $N_{55} \langle \delta_R^2 \rangle$ from unity denotes the new effect appearing in the novel formulation. The corresponding factors are given with the Fourier components of the window function, \tilde{W} , as

$$\langle \delta_R^2 \rangle = \mathcal{A} \left(\frac{4}{9} \right)^2 \int_{k_l}^{k_s} \frac{dk}{k} (kR)^4 T^2(\eta = R, k) \tilde{W}^2(R, k), \quad (2.12)$$

$$\langle (\delta_{R,R})^2 \rangle = \mathcal{A} \left(\frac{4}{9} \right)^2 \int_{k_l}^{k_s} \frac{dk}{k} \left(\frac{\partial}{\partial R} \left[(kR)^2 T(\eta = R, k) \tilde{W}(R, k) \right] \right)^2, \quad (2.13)$$

⁴The effects of the non-Gaussianity in the conventional formulation are discussed in refs. [50–56].

$$\langle \delta_R \delta_{R,R} \rangle = \mathcal{A} \left(\frac{4}{9} \right)^2 \int_{k_l}^{k_s} \frac{dk}{k} (kR)^2 T(\eta = R, k) \tilde{W}(R, k) \frac{\partial}{\partial R} \left[(kR)^2 T(\eta = R, k) \tilde{W}(R, k) \right] , \quad (2.14)$$

where we have used eq. (2.2) and introduced the transfer function for the density perturbation to take into account its subhorizon evolution, which is given with the conformal time η as [57]

$$T(\eta, k) = 3 \frac{\sin(k\eta/\sqrt{3}) - (k\eta/\sqrt{3}) \cos(k\eta/\sqrt{3})}{(k\eta/\sqrt{3})^3} . \quad (2.15)$$

This transfer function plays an important role in the case of the x -space top-hat window function because the suppression of the subhorizon contribution by the window function itself is not so strong. On the other hand, the transfer function is not important for the Gaussian and the k -space top-hat window functions since these two window functions sufficiently suppress the subhorizon contribution by themselves [40, 41], and hence we set the transfer function to unity for these two cases for clarity of expression in the rest of this paper.⁵

3 Review on window functions and their properties

In this section, we review the three commonly used window functions: (i) the Gaussian, (ii) the x -space top-hat, and (iii) the k -space top-hat window function. Following the convention in ref. [41], we define these window functions as

(i) Gaussian window function:

$$W(R, r) = \frac{1}{(\pi R^2)^{3/2}} \exp\left(-\frac{r^2}{R^2}\right) , \quad (3.1)$$

$$\tilde{W}(R, k) = \exp\left[-\frac{(kR)^2}{4}\right] , \quad (3.2)$$

(ii) x -space top-hat window function:

$$W(R, r) = \frac{3}{4\pi R^3} \Theta(R - r) , \quad (3.3)$$

$$\tilde{W}(R, k) = 3 \frac{\sin(kR) - kR \cos(kR)}{(kR)^3} , \quad (3.4)$$

(iii) k -space top-hat window function:

$$W(R, r) = \frac{\alpha^3}{2\pi^2 R^3} \frac{\sin[\alpha(r/R)] - \alpha(r/R) \cos[\alpha(r/R)]}{[\alpha(r/R)]^3} , \quad (3.5)$$

$$\tilde{W}(R, k) = \Theta\left(\frac{\alpha}{R} - k\right) , \quad (3.6)$$

where $\alpha = 2.744$ and the three window functions are defined such that $4\pi r^2 W(R, r)$, which will appear in eq. (3.11), has its peak at $r = R$ [41].⁶ All the window functions above satisfy

⁵We have numerically checked that this prescription for the transfer function hardly affects the extra factor defined in eq. (4.7).

⁶Due to this peak condition for $4\pi r^2 W(R, r)$, eqs. (3.2) and (3.6) are slightly different from the conventional window functions, used in e.g. ref. [40].

the normalization condition $\tilde{W}(R, k = 0) = 1$ in the Fourier space and the Gaussian and the x -space top-hat window function satisfy $\int d^3x W(R, |\boldsymbol{x}|) = 1$ in the real space. Substituting eqs. (3.2), (3.4), and (3.6) into eq. (2.12) and performing the variable transformation $u \equiv kR$, we can express $\langle \delta_R^2 \rangle$ for each window function as

(i) Gaussian window function:

$$\langle \delta_R^2 \rangle = \mathcal{A} \left(\frac{4}{9} \right)^2 \int_{\xi}^{s\xi} du u^3 e^{-u^2/2} = -2\mathcal{A} \left(\frac{4}{9} \right)^2 \Delta\Gamma_2 , \quad (3.7)$$

(ii) x -space top-hat window function:

$$\langle \delta_R^2 \rangle = \mathcal{A} \left(\frac{4}{9} \right)^2 \int_{\xi}^{s\xi} du u^3 \left(3 \frac{\sin u - u \cos u}{u^3} \right)^2 \left[3 \frac{\sin(u/\sqrt{3}) - (u/\sqrt{3}) \cos(u/\sqrt{3})}{(u/\sqrt{3})^3} \right]^2 , \quad (3.8)$$

(iii) k -space top-hat window function:

$$\langle \delta_R^2 \rangle = \begin{cases} \frac{\mathcal{A}}{4} \left(\frac{4}{9} \right)^2 (s^4 - 1) \xi^4 & (0 < \xi < \alpha/s) \\ \frac{\mathcal{A}}{4} \left(\frac{4}{9} \right)^2 (\alpha^4 - \xi^4) & (\alpha/s \leq \xi \leq \alpha) \\ 0 & (\xi > \alpha) \end{cases} , \quad (3.9)$$

where we have introduced $\xi \equiv k_l R$ and $s \equiv k_s/k_l$, so that $k_s R = s\xi$. Note again that we have set $T(k, \eta(= R)) = 1$ for the Gaussian and the k -space top-hat window functions for clarity. Here $\Delta\Gamma_q$ is defined as $\Delta\Gamma_q \equiv \Gamma(q, (k_s R)^2/2) - \Gamma(q, (k_l R)^2/2) = \Gamma(q, (s\xi)^2/2) - \Gamma(q, \xi^2/2)$ in terms of the incomplete gamma function,

$$\Gamma(q, x) \equiv \int_x^{\infty} dt t^{q-1} e^{-t} . \quad (3.10)$$

To see how these window functions smooth the density contrast, let us observe the relation between the traditional exponential factor $\delta_{\text{th}}^2 / \langle \delta_R^2 \rangle$ and ξ . Here, we should notice that the threshold δ_{th} also depends on the choice of the window function, as discussed in ref. [41]. Following the discussion in the reference, we assume that the threshold is given by

$$\delta_{\text{th}} = \int_0^{\infty} dr 4\pi r^2 W(R, r) \delta_c(R, r) . \quad (3.11)$$

Here we choose $\delta_c(R, r)$ as a typical density profile of the peak, which may be almost independent of the power spectrum of the perturbations [34, 41], with the numerically determined critical amplitude $A_c \simeq 1.2$ [34]:

$$\delta_c(R, r) = A_c \frac{\sin[\alpha(r/R)]}{\alpha(r/R)} . \quad (3.12)$$

The numerical results of the thresholds are listed in table 1 [41].

Figure 1 shows the behaviors of $\mathcal{A}\delta_{\text{th}}^2/\langle\delta_R^2\rangle$ at $s = 10$, for the three window functions.⁷ It is seen that all the window functions exhibit flat behaviors in $\alpha/s \lesssim \xi \lesssim 1$. The smallest flat value of $\delta_{\text{th}}^2/\langle\delta_R^2\rangle$ is obtained for the Gaussian window function ($\delta_{\text{th}}^2/\langle\delta_R^2\rangle \simeq 0.082$), while the largest one for the x -space top-hat window function ($\delta_{\text{th}}^2/\langle\delta_R^2\rangle \simeq 0.24$). The result for the k -space top-hat window function is intermediate ($\delta_{\text{th}}^2/\langle\delta_R^2\rangle \simeq 0.12$) with the cut-off at $\xi = \alpha$.

For the Gaussian window function with $\xi \gtrsim 1$, $\langle\delta_R^2\rangle$ behaves as

$$\langle\delta_R^2\rangle \simeq \mathcal{A} \left(\frac{4}{9}\right)^2 (2 + \xi^2) e^{-\xi^2/2} \quad (\xi \gtrsim 1 \text{ for Gaussian}) . \quad (3.13)$$

For the x -space top-hat window function with $\xi \gtrsim 1$, $\langle\delta_R^2\rangle$ can be expressed as

$$\begin{aligned} \langle\delta_R^2\rangle \simeq \frac{9\mathcal{A}}{2\xi^5} & \left(2\xi - 4\sin(2\xi) - 4\sqrt{3}\sin\left(\frac{2\xi}{\sqrt{3}}\right) - (3 + \sqrt{3})\sin\left[\frac{2}{3}(3 - \sqrt{3})\xi\right] \right. \\ & \left. - (3 - \sqrt{3})\sin\left[\frac{2}{3}(3 + \sqrt{3})\xi\right] \right) \quad (\xi \gtrsim 1 \text{ for } x\text{-space top-hat}) . \end{aligned} \quad (3.14)$$

On the other hand, when $\xi \lesssim \alpha/s$, $\langle\delta_R^2\rangle$ can be universally approximated as

$$\langle\delta_R^2\rangle \simeq \frac{\mathcal{A}}{4} \left(\frac{4}{9}\right)^2 (s^4 - 1)\xi^4 \quad (\xi \lesssim \alpha/s \text{ for all the window functions}) . \quad (3.15)$$

This is because all the Fourier-transformed window functions reach unity for small enough smoothing scale. Hence, the difference between the three lines in $\xi \lesssim \alpha/s$ in Figure 1 comes from the window function dependence of δ_{th} , shown in table 1.

	Gaussian	x -space top-hat	k -space top-hat
δ_{th}	0.18	0.51	0.59

Table 1. The window function dependence of the threshold δ_{th} at the horizon re-entry [41].

4 Window function dependence of the novel mass function

In this section, we see how much the extra factor $N_{55}\langle\delta_R^2\rangle$ in the novel mass function deviates from unity for each window function, which indicates the new effect from the novel mass function, as we mentioned in section 2. We also discuss the full exponential factor $N_{55}\delta_{\text{th}}^2$ comparing it with the conventional one, $\delta_{\text{th}}^2/\langle\delta_R^2\rangle$.

The factors appearing in N_{55} other than $\langle\delta_R^2\rangle$ are given by

(i) Gaussian window function:

$$\langle(\delta_{R,R})^2\rangle = \mathcal{A} \left(\frac{4}{9}\right)^2 \frac{1}{R^2} \int_{\xi}^{s\xi} du u \left(\frac{d}{du} \left[u^2 e^{-u^2/4} \right] \right)^2$$

⁷ Note that the behavior of $\langle\delta_R^2\rangle$ is almost the same for larger s . This is also true for the results given in the next section.

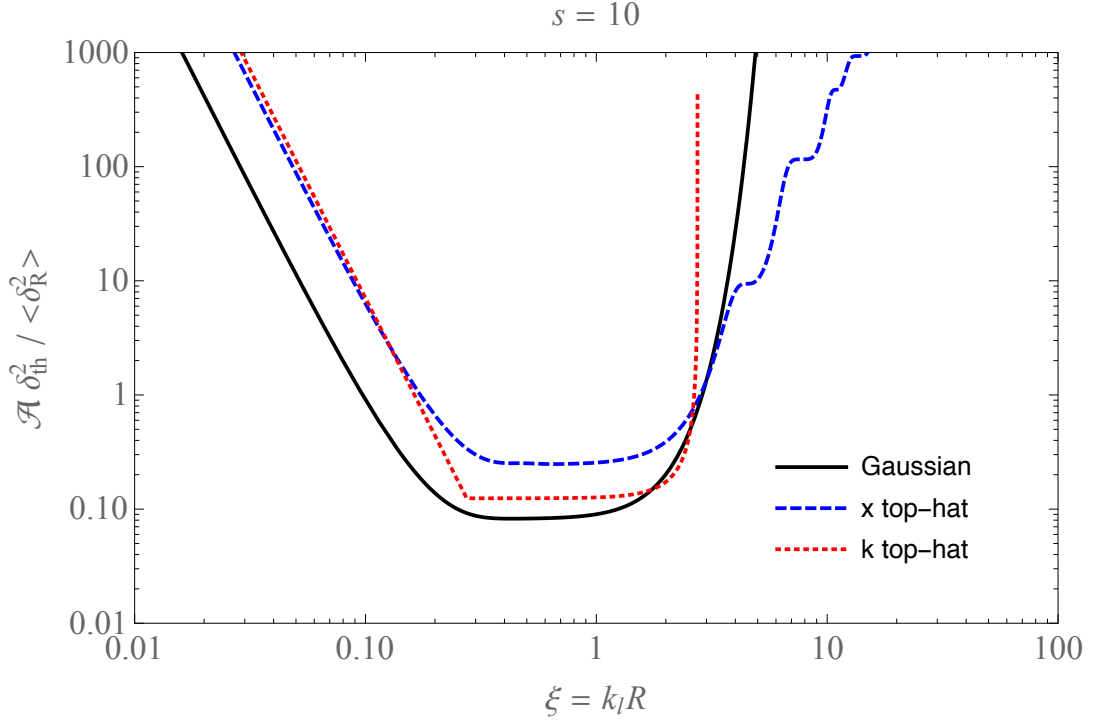


Figure 1. The behaviors of $\mathcal{A} \delta_{\text{th}}^2 / \langle \delta_R^2 \rangle$ with respect to $\xi = k_l R$ in $s = 10$.

$$= -2\mathcal{A} \left(\frac{4}{9}\right)^2 \frac{1}{R^2} [\Delta\Gamma_4 - 4(\Delta\Gamma_3 - \Delta\Gamma_2)] , \quad (4.1)$$

$$\begin{aligned} \langle \delta_R \delta_{R,R} \rangle &= \mathcal{A} \left(\frac{4}{9}\right)^2 \frac{1}{R} \int_{\xi}^{s\xi} du u^2 e^{-u^2/4} \frac{d}{du} \left[u^2 e^{-u^2/4} \right] \\ &= 2\mathcal{A} \left(\frac{4}{9}\right)^2 \frac{1}{R} (\Delta\Gamma_3 - 2\Delta\Gamma_2) , \end{aligned} \quad (4.2)$$

(ii) x -space top-hat window function:

$$\begin{aligned} \langle (\delta_{R,R})^2 \rangle &= \mathcal{A} \left(\frac{4}{9}\right)^2 \frac{1}{R^2} \int_{\xi}^{s\xi} du u \left(\frac{d}{du} \left[u^2 \cdot 3 \frac{\sin u - u \cos u}{u^3} \right. \right. \\ &\quad \left. \left. \times 3 \frac{\sin(u/\sqrt{3}) - (u/\sqrt{3}) \cos(u/\sqrt{3})}{(u/\sqrt{3})^3} \right] \right)^2 , \end{aligned} \quad (4.3)$$

$$\begin{aligned} \langle \delta_R \delta_{R,R} \rangle &= \mathcal{A} \left(\frac{4}{9}\right)^2 \frac{1}{R} \int_{\xi}^{s\xi} du u^2 \cdot 3 \frac{\sin u - u \cos u}{u^3} \cdot 3 \frac{\sin(u/\sqrt{3}) - (u/\sqrt{3}) \cos(u/\sqrt{3})}{(u/\sqrt{3})^3} \\ &\quad \times \frac{d}{du} \left[u^2 \cdot 3 \frac{\sin u - u \cos u}{u^3} \cdot 3 \frac{\sin(u/\sqrt{3}) - (u/\sqrt{3}) \cos(u/\sqrt{3})}{(u/\sqrt{3})^3} \right] , \end{aligned} \quad (4.4)$$

(iii) k -space top-hat window function:

$$\begin{aligned}
\langle (\delta_{R,R})^2 \rangle &= \mathcal{A} \left(\frac{4}{9} \right)^2 \frac{1}{R^2} \int_{\xi}^{s\xi} du u \left(\frac{d}{du} [u^2 \Theta(\alpha - u)] \right)^2 \\
&= \begin{cases} \mathcal{A} \left(\frac{4}{9} \right)^2 \frac{1}{R^2} (s^4 - 1) \xi^4 & (0 < \xi < \alpha/s) \\ \mathcal{A} \left(\frac{4}{9} \right)^2 \frac{1}{R^2} [\alpha^5 \delta_{\text{D}}(0) + (\alpha^4 - \xi^4) - 4\alpha^4 \Theta(0)] & (\alpha/s \leq \xi \leq \alpha) \\ 0 & (\xi > \alpha) \end{cases}, \quad (4.5) \\
\langle \delta_R \delta_{R,R} \rangle &= \mathcal{A} \left(\frac{4}{9} \right)^2 \frac{1}{R} \int_{\xi}^{s\xi} du u^2 \Theta(\alpha - u) \frac{d}{du} [u^2 \Theta(\alpha - u)] \\
&= \begin{cases} \frac{\mathcal{A}}{2} \left(\frac{4}{9} \right)^2 \frac{1}{R} (s^4 - 1) \xi^4 & (0 < \xi < \alpha/s) \\ \frac{\mathcal{A}}{2} \left(\frac{4}{9} \right)^2 \frac{1}{R} [(\alpha^4 - \xi^4) - 2\alpha^4 \Theta(0)] & (\alpha/s \leq \xi \leq \alpha) \\ 0 & (\xi > \alpha) \end{cases}. \quad (4.6)
\end{aligned}$$

Note that, for $\xi < \alpha/s$, the k -space top-hat window function yields $\langle \delta_R^2 \rangle \langle (\delta_{R,R})^2 \rangle - \langle \delta_R \delta_{R,R} \rangle^2 = 0$ and hence we cannot define N_{55} . In this regime, $\delta_{R,R} = 2\delta_R/R$ holds for the k -space top-hat window function, which means $\delta_R > \delta_{\text{th}}$ and $\delta_{R,R} = 0$ cannot be satisfied at the same time. Therefore, we can conclude that PBHs are not produced in $\xi < \alpha/s$ for the k -space top-hat window function. The similar issue, the impossibility of defining N_{55} , also arises for $\xi > \alpha$, but the fact that $\langle \delta_R^2 \rangle = 0$ implies that, again, no PBH formation occurs in the regime.⁸ Therefore, for the k -space top-hat window function, PBH production is allowed only in $\alpha/s < \xi < \alpha$ and, in this region, the divergence of $\langle (\delta_{R,R})^2 \rangle$ leads to $N_{55} \langle \delta_R^2 \rangle = 1$ and $N_{55} \delta_{\text{th}}^2 = \delta_{\text{th}}^2 / \langle \delta_R^2 \rangle$, giving the same exponential factor as the one for the conventional mass function.

Figure 2 shows the extra factor in the exponent of the novel mass function, given by

$$N_{55} \langle \delta_R^2 \rangle = \frac{\langle \delta_R^2 \rangle \langle (\delta_{R,R})^2 \rangle}{\langle \delta_R^2 \rangle \langle (\delta_{R,R})^2 \rangle - \langle \delta_R \delta_{R,R} \rangle^2}. \quad (4.7)$$

As mentioned above, the result from the k -space top-hat window function agrees to the conventional result due to the divergence of $\langle (\delta_{R,R})^2 \rangle$. The other two window functions also give the same magnitudes as the conventional ones, $N_{55} \langle \delta_R^2 \rangle \simeq 1$, in $\alpha/s \lesssim \xi \lesssim 1$ due to the fact that $\langle \delta_R^2 \rangle \langle (\delta_{R,R})^2 \rangle \gg \langle \delta_R \delta_{R,R} \rangle^2$ in the regime, which means that δ_R and $\delta_{R,R}$ are hardly correlated. On the other hand, the factor from the Gaussian window function is much larger than unity in $\xi \lesssim \alpha/s$ or $\xi \gtrsim 1$, indicating less PBH formation. For the x -space top-hat window function, while the extra factor behaves similarly to the Gaussian window case in $\xi \lesssim \alpha/s$, it fluctuates a little in $\xi \sim \mathcal{O}(1)$ and reaches unity again in $\xi \gg 1$.

⁸ Note that the behaviors of the exponential factor in $\xi < \alpha/s$ or $\xi > \alpha$ for the k -space top-hat window function are the consequence of the exact top-hat power spectrum, defined in eq. (2.4). If we assume the additional power spectrum that is small but scale invariant as $\mathcal{P}_{\mathcal{R}} = \mathcal{A} \Theta(k - k_l) \Theta(-k + k_s) + \mathcal{B}$ ($\mathcal{B} \ll \mathcal{A}$), $\langle (\delta_{R,R})^2 \rangle$ diverges for all ξ , which leads to the same exponential factor as the conventional one regardless of ξ .

Figure 3 shows the full exponential factor in the novel mass function, given by

$$N_{55}\delta_{\text{th}}^2 = \frac{\langle(\delta_{R,R})^2\rangle}{\langle\delta_R^2\rangle\langle(\delta_{R,R})^2\rangle - \langle\delta_R\delta_{R,R}\rangle^2}\delta_{\text{th}}^2. \quad (4.8)$$

From this figure, we can see that, for $\alpha/s \lesssim \xi \lesssim 1$, the novel mass function predicts the same outcome as the conventional one for all the window functions, as long as we focus on the exponential factor. This is true even for the result with the x -space top-hat window function in $\xi \gtrsim 1$. On the other hand, the results with the Gaussian window function in $\xi \lesssim \alpha/s$ or $\xi \gtrsim 1$ and the x -space top-hat window function in $\xi \lesssim \alpha/s$ predict the larger exponent compared to the corresponding factors in the conventional formulation, which means the suppression of the PBH abundance in the regimes and leads to narrow PBH mass spectra.

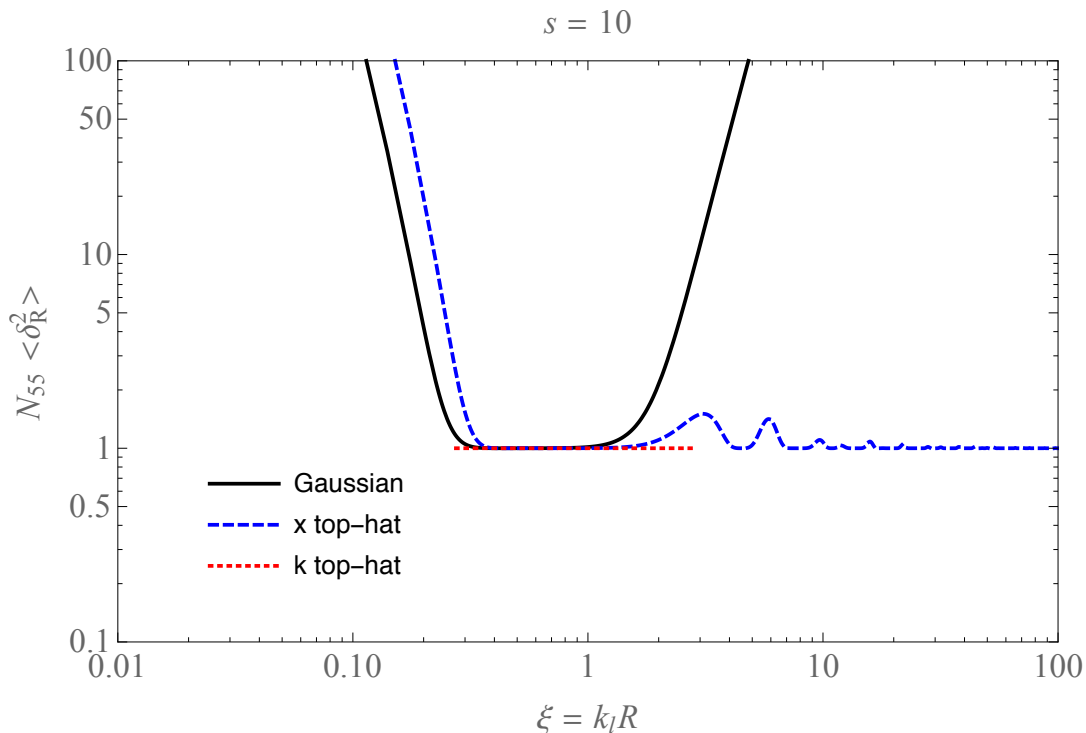


Figure 2. The behavior of the extra factor in the exponential factor of the novel mass function, given in eq. (4.7), with respect to $\xi = k_l R$ for $s = 10$.

5 Conclusion and discussion

The relation between the power spectrum of the curvature perturbations and the mass function of PBHs has been studied by many authors. Also, the window function dependence of the mass function has been discussed in refs. [40, 41]. Recently, the novel mass function has been proposed in ref. [38] with the additional criterion that PBH formation should be related to the smoothing scale at which the density contrast becomes maximum. This novel formulation is free from the questionable assumption in the conventional mass formulation

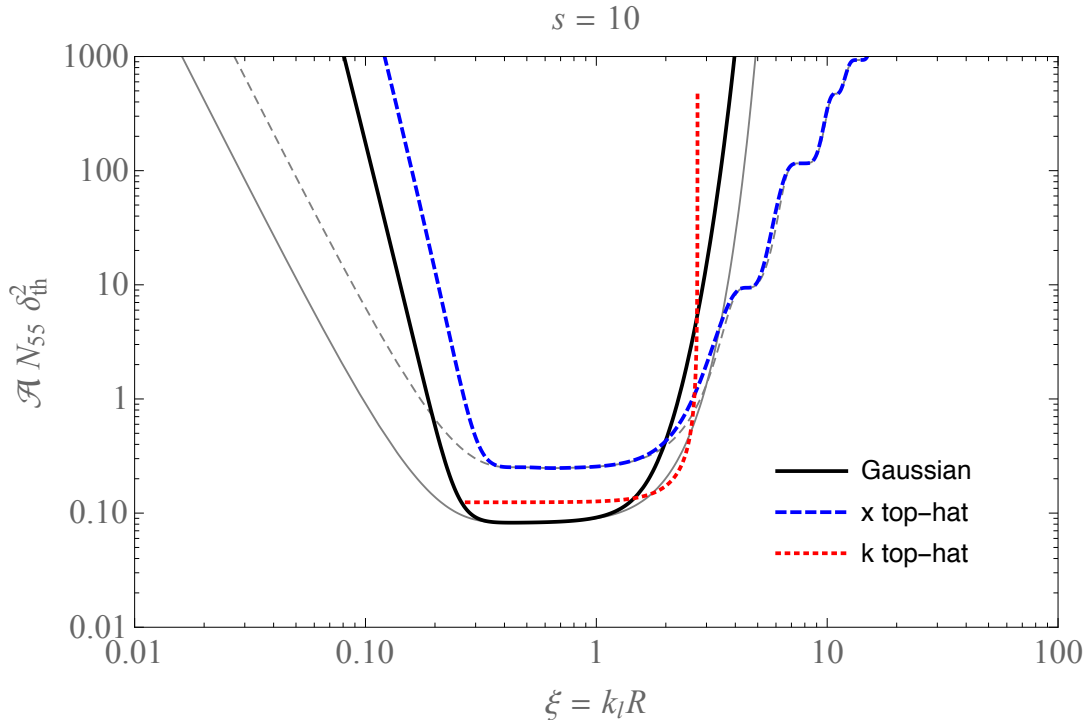


Figure 3. Window function dependence of the exponential factor of the novel mass function, given in eq. (4.8), with respect to $\xi = k_l R$ for $s = 10$. For comparison, we also show the conventional factors $\mathcal{A} \delta_{\text{th}}^2 / \langle \delta_R^2 \rangle$ from the Gaussian window function (thin gray solid) and the x -space top-hat window function (thin gray dashed), which are the same plots as in figure 1.

and therefore is superior to the conventional one in some sense. However, the novel mass function still has the uncertainties originating from the choice of the window function.

In this paper, we have revisited the window function dependence of the PBH mass function, especially focusing on the exponential factor of the mass function, which is a decisive quantity to determine the abundance of PBHs. We have used the smoothed density contrast δ_R to describe PBH formation with the top-hat power spectrum $\mathcal{P}_{\mathcal{R}} = \mathcal{A} \Theta(k - k_l) \Theta(-k + k_s)$ and considered the three kinds of window functions: the Gaussian, the x -space top-hat, and the k -space top-hat window functions. As a result, we have found that all the window functions reproduce the exponential factors of the conventional mass function around the top-hat region ($\alpha/s \lesssim \xi \lesssim 1$). On the other hand, the Gaussian window function gives the larger exponent than the conventional one in $\xi \lesssim \alpha/s$ or $\xi \gtrsim 1$, and also the x -space top-hat window function does in $\xi \lesssim \alpha/s$. This means that the novel mass function predicts the narrower PBH mass spectrum compared to the conventional one, which is consistent with the result in ref. [39] which is based on x -space top-hat smoothing of other control variables than ours.

Acknowledgments

We thank Teruaki Suyama and Shuichiro Yokoyama for useful communications. This work was partially supported by JSPS KAKENHI Grant Numbers, 15H02082 and 20H05248.

A The novel mass function in the 4-dimensional spacetime

In this section, we derive the expression of $I(M)$ in the full three-dimensional space with additional variable R , extending the one-dimensional analysis of [38]. Similar four-dimensional analysis with different variables has been done in [39]. As we mentioned in eq. (2.8), $I(M)$ in the 4-dimensional ‘‘spacetime’’ is defined as

$$I(M) \equiv \left\langle |\det H| \Theta(\delta_R - \delta_{\text{th}}) \prod_{\alpha=1}^4 \delta_{\text{D}}(\delta_{R,\alpha}) \Theta(-\lambda_\alpha) \right\rangle, \quad (\text{A.1})$$

where the Hesse matrix H can be explicitly written as

$$H = \begin{pmatrix} \delta_{R,xx} & \delta_{R,xy} & \delta_{R,xz} & \delta_{R,xR} \\ \delta_{R,yx} & \delta_{R,yy} & \delta_{R,yz} & \delta_{R,yR} \\ \delta_{R,zx} & \delta_{R,zy} & \delta_{R,zz} & \delta_{R,zR} \\ \delta_{R,Rx} & \delta_{R,Ry} & \delta_{R,Rz} & \delta_{R,RR} \end{pmatrix}. \quad (\text{A.2})$$

Here, we transform the delta function and the Heaviside step function as

$$\begin{aligned} \delta_{\text{D}}(\delta_{R,x}) &= \int \frac{d\eta_1}{2\pi} e^{i\eta_1 \delta_{R,x}}, \\ \delta_{\text{D}}(\delta_{R,y}) &= \int \frac{d\eta_2}{2\pi} e^{i\eta_2 \delta_{R,y}}, \\ \delta_{\text{D}}(\delta_{R,z}) &= \int \frac{d\eta_3}{2\pi} e^{i\eta_3 \delta_{R,z}}, \\ \delta_{\text{D}}(\delta_{R,R}) &= \int \frac{d\eta_4}{2\pi} e^{i\eta_4 \delta_{R,R}}, \\ \Theta(\delta_R - \delta_{\text{th}}) &= \int_{\delta_{\text{th}}}^{\infty} d\theta \int \frac{d\eta_5}{2\pi} e^{i\eta_5(\delta_R - \theta)}. \end{aligned} \quad (\text{A.3})$$

In addition, as done in ref. [38], we assume $\Theta(-\lambda_\alpha) = 1$ because PBHs are produced by high peaks ($\delta_{\text{th}} \gg \delta_R$). Then, we can rewrite eq. (A.1) as

$$I(M) = \left[\prod_{i=1}^5 \int \frac{d\eta_i}{2\pi} \right] \int_{\delta_{\text{th}}}^{\infty} d\theta e^{-i\eta_5 \theta} \left\langle |\det H| e^{i(\eta_1 \delta_{R,x} + \eta_2 \delta_{R,y} + \eta_3 \delta_{R,z} + \eta_4 \delta_{R,R} + \eta_5 \delta_R)} \right\rangle. \quad (\text{A.4})$$

To perform the integral, we use the following relation: (x_i follow the Gaussian distribution with zero mean and their covariances are given as $\langle x_i x_j \rangle = P_{ij}$)

$$\begin{aligned} \langle x_i x_j x_k x_l e^{i u_m x_m} \rangle &= \left\langle x_i x_j x_k x_l \left[1 - \frac{1}{2!} (u_k x_k)^2 + \frac{1}{4!} (u_k x_k)^4 - \frac{1}{6!} (u_k x_k)^6 + \dots \right] \right\rangle \\ &= [P_{ij} P_{kl} + P_{ik} P_{jl} + P_{il} P_{jk} \\ &\quad - (P_{ij} P_{km} u_m P_{ln} u_n + P_{ik} P_{jm} u_m P_{ln} u_n + P_{il} P_{jm} u_m P_{kn} u_n \\ &\quad + P_{jk} P_{im} u_m P_{ln} u_n + P_{jl} P_{im} u_m P_{kn} u_n + P_{kl} P_{im} u_m P_{jn} u_n) \\ &\quad + P_{im} u_m P_{jn} u_n P_{ks} u_s P_{lt} u_t] \exp\left(-\frac{1}{2} P_{mn} u_m u_n\right), \end{aligned} \quad (\text{A.5})$$

where we have killed the irrelevant terms, which are composed of odd-numbered x_i , in the first equality because such terms become zero under the Gaussian distribution. Using this relation, we can rewrite eq. (A.4) as

$$\begin{aligned}
I(M) &= \int_{\delta_{\text{th}}}^{\infty} d\theta \left[\prod_{i=1}^5 \int \frac{d\eta_i}{2\pi} \right] (A + B_{ij}\eta_i\eta_j + C_{ijkl}\eta_i\eta_j\eta_k\eta_l) \exp\left(-\frac{1}{2}L_{ij}\eta_i\eta_j + iv_i\eta_i\right) \\
&= \frac{1}{\sqrt{\det(2\pi L)}} \int_{\delta_{\text{th}}}^{\infty} d\theta [A + B_{ij}N_{ij} - B_{ij}N_{ik}N_{jl}v_kv_l \\
&\quad + 3C_{ijkl}N_{ij}N_{kl} - 6C_{ijkl}N_{ij}N_{km}v_mN_{lm}v_m \\
&\quad + C_{ijkl}N_{im}v_mN_{jm}v_mN_{km}v_mN_{lm}v_m] \exp\left(-\frac{1}{2}N_{ij}v_iv_j\right) \\
&= \frac{1}{\sqrt{\det(2\pi L)}} \sqrt{\frac{2}{N_{55}}} \\
&\quad \times \left[\left(A + B_{ij}N_{ij} + 3C_{ijkl}N_{ij}N_{kl} - \frac{(B_{ij} + 6C_{ijkl}N_{kl})N_{i5}N_{j5}}{N_{55}} + \frac{3C_{ijkl}N_{i5}N_{j5}N_{k5}N_{l5}}{N_{55}^2} \right) \right. \\
&\quad \times \frac{\sqrt{\pi}}{2} \text{erfc}\left(\sqrt{\frac{N_{55}}{2}}\delta_{\text{th}}\right) \\
&\quad + \frac{\delta_{\text{th}}}{\sqrt{2N_{55}}} \left((B_{ij} + 6C_{ijkl}N_{kl})N_{i5}N_{j5} + \frac{\delta_{\text{th}}(3 + N_{55}\delta_{\text{th}}^2)C_{ijkl}N_{i5}N_{j5}N_{k5}N_{l5}}{N_{55}} \right) \\
&\quad \left. \times \exp\left(-\frac{N_{55}}{2}\delta_{\text{th}}^2\right) \right], \tag{A.6}
\end{aligned}$$

where L_{ij} is defined in eq. (2.10), v_i is given as $v_i = (0, 0, 0, 0, -\theta)$ and N_{ij} is the inverse matrix of L_{ij} , given as

$$N = \begin{pmatrix} N_{11} & & & & \\ & N_{22} & & & \\ & & N_{33} & & \\ & & & N_{44} & N_{45} \\ & & & N_{54} & N_{55} \end{pmatrix}, \tag{A.7}$$

where

$$\begin{aligned}
\begin{pmatrix} N_{11} & & \\ & N_{22} & \\ & & N_{33} \end{pmatrix} &= \begin{pmatrix} \frac{1}{\langle(\delta_{R,x})^2\rangle} & & \\ & \frac{1}{\langle(\delta_{R,y})^2\rangle} & \\ & & \frac{1}{\langle(\delta_{R,z})^2\rangle} \end{pmatrix}, \tag{A.8} \\
\begin{pmatrix} N_{44} & N_{45} \\ N_{54} & N_{55} \end{pmatrix} &= \begin{pmatrix} \frac{\langle\delta_R^2\rangle}{\langle\delta_R^2\rangle\langle(\delta_{R,R})^2\rangle - \langle\delta_{R,R}\delta_R\rangle^2} & -\frac{\langle\delta_{R,R}\delta_R\rangle}{\langle\delta_R^2\rangle\langle(\delta_{R,R})^2\rangle - \langle\delta_{R,R}\delta_R\rangle^2} \\ -\frac{\langle\delta_{R,R}\delta_R\rangle}{\langle\delta_R^2\rangle\langle(\delta_{R,R})^2\rangle - \langle\delta_{R,R}\delta_R\rangle^2} & \frac{\langle(\delta_{R,R})^2\rangle}{\langle\delta_R^2\rangle\langle(\delta_{R,R})^2\rangle - \langle\delta_{R,R}\delta_R\rangle^2} \end{pmatrix}. \tag{A.9}
\end{aligned}$$

A in eq. (A.6) is given as

$$A = (\langle \delta_{R,RR} \delta_{R,xx} \rangle - \langle (\delta_{R,Rx})^2 \rangle) (\langle \delta_{R,yy} \delta_{R,zz} \rangle - \langle (\delta_{R,yz})^2 \rangle) + (x \leftrightarrow y) + (x \leftrightarrow z), \quad (\text{A.10})$$

B_{ij} is the 5×5 symmetric and block diagonal matrix whose nonzero components are given by

$$B_{11} = \langle \delta_{R,x} \delta_{R,Rx} \rangle^2 (\langle \delta_{R,yy} \delta_{R,zz} \rangle - \langle \delta_{R,yz} \rangle^2), \quad (\text{A.11})$$

$$B_{22} = \langle \delta_{R,y} \delta_{R,Ry} \rangle^2 (\langle \delta_{R,zz} \delta_{R,xx} \rangle - \langle \delta_{R,zx} \rangle^2), \quad (\text{A.12})$$

$$B_{33} = \langle \delta_{R,z} \delta_{R,Rz} \rangle^2 (\langle \delta_{R,xx} \delta_{R,yy} \rangle - \langle \delta_{R,xy} \rangle^2), \quad (\text{A.13})$$

$$\begin{aligned} -B_{44} = & \left[\langle \delta_{R,R} \delta_{R,RR} \rangle \langle \delta_{R,R} \delta_{R,xx} \rangle (\langle \delta_{R,yy} \delta_{R,zz} \rangle - \langle \delta_{R,yz} \rangle^2) \right. \\ & \left. + \langle \delta_{R,R} \delta_{R,yy} \rangle \langle \delta_{R,R} \delta_{R,zz} \rangle (\langle \delta_{R,RR} \delta_{R,xx} \rangle - \langle \delta_{R,Rx} \rangle^2) \right] \\ & + (x \leftrightarrow y) + (x \leftrightarrow z), \end{aligned} \quad (\text{A.14})$$

$$\begin{aligned} -B_{55} = & \left[\langle \delta_R \delta_{R,RR} \rangle \langle \delta_R \delta_{R,xx} \rangle (\langle \delta_{R,yy} \delta_{R,zz} \rangle - \langle \delta_{R,yz} \rangle^2) \right. \\ & \left. + \langle \delta_R \delta_{R,yy} \rangle \langle \delta_R \delta_{R,zz} \rangle (\langle \delta_{R,RR} \delta_{R,xx} \rangle - \langle \delta_{R,Rx} \rangle^2) \right] \\ & + (x \leftrightarrow y) + (x \leftrightarrow z), \end{aligned} \quad (\text{A.15})$$

$$\begin{aligned} -2B_{45} = & \left[(\langle \delta_R \delta_{R,RR} \rangle \langle \delta_{R,R} \delta_{R,xx} \rangle + \langle \delta_R \delta_{R,xx} \rangle \langle \delta_{R,R} \delta_{R,RR} \rangle) (\langle \delta_{R,yy} \delta_{R,zz} \rangle - \langle \delta_{R,yz} \rangle^2) \right. \\ & \left. + (\langle \delta_R \delta_{R,yy} \rangle \langle \delta_{R,R} \delta_{R,zz} \rangle + \langle \delta_R \delta_{R,zz} \rangle \langle \delta_{R,R} \delta_{R,yy} \rangle) (\langle \delta_{R,RR} \delta_{R,xx} \rangle - \langle \delta_{R,Rx} \rangle^2) \right] \\ & + (x \leftrightarrow y) + (x \leftrightarrow z), \end{aligned} \quad (\text{A.16})$$

and C_{ijkl} is the tensor invariant under an arbitrary exchange between $i, j, k,$ and $l \in \{1, \dots, 5\}$ whose nonzero components are given by (for $i \leq j \leq k \leq l$)

$$-6C_{1144} = \langle \delta_{R,x} \delta_{R,Rx} \rangle^2 \langle \delta_{R,R} \delta_{R,yy} \rangle \langle \delta_{R,R} \delta_{R,zz} \rangle, \quad (\text{A.17})$$

$$-6C_{2244} = \langle \delta_{R,y} \delta_{R,Ry} \rangle^2 \langle \delta_{R,R} \delta_{R,zz} \rangle \langle \delta_{R,R} \delta_{R,xx} \rangle, \quad (\text{A.18})$$

$$-6C_{3344} = \langle \delta_{R,z} \delta_{R,Rz} \rangle^2 \langle \delta_{R,R} \delta_{R,xx} \rangle \langle \delta_{R,R} \delta_{R,yy} \rangle, \quad (\text{A.19})$$

$$-6C_{1155} = \langle \delta_{R,x} \delta_{R,Rx} \rangle^2 \langle \delta_R \delta_{R,yy} \rangle \langle \delta_R \delta_{R,zz} \rangle, \quad (\text{A.20})$$

$$-6C_{2244} = \langle \delta_{R,y} \delta_{R,Ry} \rangle^2 \langle \delta_R \delta_{R,zz} \rangle \langle \delta_R \delta_{R,xx} \rangle, \quad (\text{A.21})$$

$$-6C_{3344} = \langle \delta_{R,z} \delta_{R,Rz} \rangle^2 \langle \delta_R \delta_{R,xx} \rangle \langle \delta_R \delta_{R,yy} \rangle, \quad (\text{A.22})$$

$$-12C_{1145} = \langle \delta_{R,x} \delta_{R,Rx} \rangle^2 (\langle \delta_R \delta_{R,yy} \rangle \langle \delta_{R,R} \delta_{R,zz} \rangle + \langle \delta_R \delta_{R,zz} \rangle \langle \delta_{R,R} \delta_{R,yy} \rangle), \quad (\text{A.23})$$

$$-12C_{2245} = \langle \delta_{R,y} \delta_{R,Ry} \rangle^2 (\langle \delta_R \delta_{R,zz} \rangle \langle \delta_{R,R} \delta_{R,xx} \rangle + \langle \delta_R \delta_{R,xx} \rangle \langle \delta_{R,R} \delta_{R,zz} \rangle), \quad (\text{A.24})$$

$$-12C_{1145} = \langle \delta_{R,z} \delta_{R,Rz} \rangle^2 (\langle \delta_R \delta_{R,xx} \rangle \langle \delta_{R,R} \delta_{R,yy} \rangle + \langle \delta_R \delta_{R,yy} \rangle \langle \delta_{R,R} \delta_{R,xx} \rangle), \quad (\text{A.25})$$

$$C_{4444} = \langle \delta_{R,R} \delta_{R,RR} \rangle \langle \delta_{R,R} \delta_{R,xx} \rangle \langle \delta_{R,R} \delta_{R,yy} \rangle \langle \delta_{R,R} \delta_{R,zz} \rangle, \quad (\text{A.26})$$

$$C_{5555} = \langle \delta_R \delta_{R,RR} \rangle \langle \delta_R \delta_{R,xx} \rangle \langle \delta_R \delta_{R,yy} \rangle \langle \delta_R \delta_{R,zz} \rangle, \quad (\text{A.27})$$

$$\begin{aligned} 6C_{4455} = & \langle \delta_R \delta_{R,RR} \rangle [\langle \delta_R \delta_{R,xx} \rangle \langle \delta_{R,R} \delta_{R,yy} \rangle \langle \delta_{R,R} \delta_{R,zz} \rangle + (x \leftrightarrow y) + (x \leftrightarrow z)] \\ & + \langle \delta_{R,R} \delta_{R,RR} \rangle [\langle \delta_{R,R} \delta_{R,xx} \rangle \langle \delta_R \delta_{R,yy} \rangle \langle \delta_R \delta_{R,zz} \rangle + (x \leftrightarrow y) + (x \leftrightarrow z)], \end{aligned} \quad (\text{A.28})$$

$$4C_{4445} = \langle \delta_R \delta_{R,RR} \rangle \langle \delta_{R,R} \delta_{R,xx} \rangle \langle \delta_{R,R} \delta_{R,yy} \rangle \langle \delta_{R,R} \delta_{R,zz} \rangle$$

$$+ \langle \delta_{R,R} \delta_{R,RR} \rangle [\langle \delta_R \delta_{R,xx} \rangle \langle \delta_{R,R} \delta_{R,yy} \rangle \langle \delta_{R,R} \delta_{R,zz} \rangle + (x \leftrightarrow y) + (x \leftrightarrow z)] , \quad (\text{A.29})$$

$$4C_{4555} = \langle \delta_{R,R} \delta_{R,RR} \rangle \langle \delta_R \delta_{R,xx} \rangle \langle \delta_R \delta_{R,yy} \rangle \langle \delta_R \delta_{R,zz} \rangle \\ + \langle \delta_R \delta_{R,RR} \rangle [\langle \delta_{R,R} \delta_{R,xx} \rangle \langle \delta_R \delta_{R,yy} \rangle \langle \delta_R \delta_{R,zz} \rangle + (x \leftrightarrow y) + (x \leftrightarrow z)] . \quad (\text{A.30})$$

References

- [1] Ya. B. Zel’dovich and I. D. Novikov. The Hypothesis of Cores Retarded during Expansion and the Hot Cosmological Model. *Sov. Astron.*, Vol. 10, pp. 602–603, 1967.
- [2] S. Hawking. Gravitationally collapsed objects of very low mass. *Mon. Not. Roy. Astron. Soc.*, Vol. 152, p. 75, 1971.
- [3] B. J. Carr and S. W. Hawking. Black Holes in the Early Universe. *Monthly Notices of the Royal Astronomical Society*, Vol. 168, No. 2, pp. 399–415, 08 1974.
- [4] B. J. Carr. The primordial black hole mass spectrum. *ApJ*, Vol. 201, pp. 1–19, October 1975.
- [5] Ya. B. Zel’dovich, A. A. Starobinskii, M. I. Khlopov, and V. M. Chechetkin. Primordial black holes and the deuterium problem. *Pisma Astron. Zh.*, Vol. 3, pp. 208–211, 1977. [*Sov. Astron. Lett.* **3**, 110 (1977).].
- [6] D. K. Nadezhin, I. D. Novikov, and A. G. Polnarev. The hydrodynamics of primordial black hole formation. *Sov. Astron.*, Vol. 22, pp. 129–138, 1978.
- [7] K. Kohri and J. Yokoyama. Primordial black holes and primordial nucleosynthesis: Effects of hadron injection from low mass holes. *Phys. Rev.*, Vol. D61, p. 023501, 1999.
- [8] B. J. Carr, K. Kohri, Y. Sendouda, and J. Yokoyama. New cosmological constraints on primordial black holes. *Phys. Rev.*, Vol. D81, p. 104019, 2010.
- [9] H. Kim and C. H. Lee. Constraints on the spectral index from primordial black holes. *Phys. Rev. D*, Vol. 54, pp. 6001–6007, Nov 1996.
- [10] M. Drees and E. Erfani. Running spectral index and formation of primordial black hole in single field inflation models. *Journal of Cosmology and Astroparticle Physics*, Vol. 2012, No. 01, pp. 035–035, jan 2012.
- [11] B. C. Lacki and J. F. Beacom. PRIMORDIAL BLACK HOLES AS DARK MATTER: ALMOST ALL OR ALMOST NOTHING. *The Astrophysical Journal*, Vol. 720, No. 1, pp. L67–L71, aug 2010.
- [12] B. J. Carr, F. Kühnel, and M. Sandstad. Primordial black holes as dark matter. *Phys. Rev. D*, Vol. 94, p. 083504, Oct 2016.
- [13] S. Bird, I. Cholis, J. B. Muñoz, Y. Ali-Haïmoud, M. Kamionkowski, E. D. Kovetz, A. Raccanelli, and A. G. Riess. Did LIGO detect dark matter? *Phys. Rev. Lett.*, Vol. 116, No. 20, p. 201301, 2016.
- [14] S. Clesse and J. García-Bellido. The clustering of massive Primordial Black Holes as Dark Matter: measuring their mass distribution with Advanced LIGO. *Phys. Dark Univ.*, Vol. 15, pp. 142–147, 2017.
- [15] M. Sasaki, T. Suyama, T. Tanaka, and S. Yokoyama. Primordial Black Hole Scenario for the Gravitational-Wave Event GW150914. *Phys. Rev. Lett.*, Vol. 117, No. 6, p. 061101, 2016.
- [16] K. Inomata, M. Kawasaki, K. Mukaida, Y. Tada, and T. Yanagida. Inflationary primordial black holes for the LIGO gravitational wave events and pulsar timing array experiments. *Phys. Rev.*, Vol. D95, No. 12, p. 123510, 2017.
- [17] K. Inomata, M. Kawasaki, K. Mukaida, Y. Tada, and T. Yanagida. Inflationary Primordial Black Holes as All Dark Matter. *Phys. Rev.*, Vol. D96, No. 4, p. 043504, 2017.

- [18] K. Inomata, M. Kawasaki, K. Mukaida, and T. Yanagida. Double inflation as a single origin of primordial black holes for all dark matter and LIGO observations. *Phys. Rev.*, Vol. D97, No. 4, p. 043514, 2018.
- [19] B. J. Carr. Primordial black holes as dark matter and generators of cosmic structure. In Rouven Essig, Jonathan Feng, and Kathryn Zurek, editors, *Illuminating Dark Matter*, pp. 29–39, Cham, 2019. Springer International Publishing.
- [20] B. J. Carr and J. E. Lidsey. Primordial black holes and generalized constraints on chaotic inflation. *Phys. Rev. D*, Vol. 48, pp. 543–553, 1993.
- [21] B. J. Carr, J. H. Gilbert, and J. E. Lidsey. Black hole relics and inflation: Limits on blue perturbation spectra. *Phys. Rev. D*, Vol. 50, pp. 4853–4867, 1994.
- [22] A. S. Josan, A. M. Green, and K. A. Malik. Generalised constraints on the curvature perturbation from primordial black holes. *Phys. Rev. D*, Vol. 79, p. 103520, 2009.
- [23] P. S. Cole and C. T. Byrnes. Extreme scenarios: the tightest possible constraints on the power spectrum due to primordial black holes. *JCAP*, Vol. 02, p. 019, 2018.
- [24] B. J. Carr, T. Tenkanen, and V. Vaskonen. Primordial black holes from inflaton and spectator field perturbations in a matter-dominated era. *Phys. Rev. D*, Vol. 96, No. 6, p. 063507, 2017.
- [25] I. Dalianis. Constraints on the curvature power spectrum from primordial black hole evaporation. *JCAP*, Vol. 08, p. 032, 2019.
- [26] G. Sato-Polito, E. D. Kovetz, and M. Kamionkowski. Constraints on the primordial curvature power spectrum from primordial black holes. *Phys. Rev. D*, Vol. 100, No. 6, p. 063521, 2019.
- [27] A. Kalaja, N. Bellomo, N. Bartolo, D. Bertacca, S. Matarrese, I. Musco, A. Raccanelli, and L. Verde. From Primordial Black Holes Abundance to Primordial Curvature Power Spectrum (and back). *JCAP*, Vol. 10, p. 031, 2019.
- [28] M. Sasaki, T. Suyama, T. Tanaka, and S. Yokoyama. Primordial black holes—perspectives in gravitational wave astronomy. *Class. Quant. Grav.*, Vol. 35, No. 6, p. 063001, 2018.
- [29] B. J. Carr, K. Kohri, Y. Sendouda, and J. Yokoyama. Constraints on Primordial Black Holes. 2020.
- [30] Hee Il Kim and Chul H. Lee. Constraints on the spectral index from primordial black holes. *Phys. Rev. D*, Vol. 54, pp. 6001–6007, 1996.
- [31] A. M. Green, A. R. Liddle, K. A. Malik, and M. Sasaki. New calculation of the mass fraction of primordial black holes. *Phys. Rev. D*, Vol. 70, p. 041502, Aug 2004.
- [32] S. Young, C. T. Byrnes, and M. Sasaki. Calculating the mass fraction of primordial black holes. *Journal of Cosmology and Astroparticle Physics*, Vol. 2014, No. 07, pp. 045–045, jul 2014.
- [33] C. M. Yoo, T. Harada, J. Garriga, and K. Kohri. Primordial black hole abundance from random Gaussian curvature perturbations and a local density threshold. *PTEP*, Vol. 2018, No. 12, p. 123E01, 2018.
- [34] C. Germani and I. Musco. Abundance of primordial black holes depends on the shape of the inflationary power spectrum. *Phys. Rev. Lett.*, Vol. 122, p. 141302, Apr 2019.
- [35] V. Atal and C. Germani. The role of non-gaussianities in Primordial Black Hole formation. *Phys. Dark Univ.*, Vol. 24, p. 100275, 2019.
- [36] W. H Press and P. Schechter. Formation of galaxies and clusters of galaxies by self-similar gravitational condensation. *The Astrophysical Journal*, Vol. 187, pp. 425–438, 1974.
- [37] J. M. Bardeen, J. R. Bond, N. Kaiser, and A. S. Szalay. The Statistics of Peaks of Gaussian Random Fields. *Apj*, Vol. 304, p. 15, May 1986.

- [38] T. Suyama and S. Yokoyama. A novel formulation of the primordial black hole mass function. *Progress of Theoretical and Experimental Physics*, Vol. 2020, No. 2, 02 2020. 023E03.
- [39] C. Germani and R. K. Sheth. Nonlinear statistics of primordial black holes from Gaussian curvature perturbations. *Phys. Rev. D*, Vol. 101, No. 6, p. 063520, 2020.
- [40] K. Ando, K. Inomata, and M. Kawasaki. Primordial black holes and uncertainties in the choice of the window function. *Phys. Rev. D*, Vol. 97, p. 103528, May 2018.
- [41] S. Young. The primordial black hole formation criterion re-examined: Parametrisation, timing and the choice of window function. *International Journal of Modern Physics D*, Vol. 29, No. 02, p. 2030002, 2020.
- [42] M. Kawasaki and H. Nakatsuka. Effect of nonlinearity between density and curvature perturbations on the primordial black hole formation. *Phys. Rev. D*, Vol. 99, No. 12, p. 123501, 2019.
- [43] V. De Luca, G. Franciolini, A. Kehagias, M. Peloso, A. Riotto, and C. Unal. The Ineludible non-Gaussianity of the Primordial Black Hole Abundance. *JCAP*, Vol. 07, p. 048, 2019.
- [44] S. Young, I. Musco, and C. T. Byrnes. Primordial black hole formation and abundance: contribution from the non-linear relation between the density and curvature perturbation. *JCAP*, Vol. 11, p. 012, 2019.
- [45] R. Mahbub. Impact of nonlinear overdensity statistics on primordial black hole abundance. 5 2020.
- [46] J. C. Niemeyer and K. Jedamzik. Near-critical gravitational collapse and the initial mass function of primordial black holes. *Phys. Rev. Lett.*, Vol. 80, pp. 5481–5484, 1998.
- [47] J. C. Niemeyer. Numerical investigation of the threshold for primordial black hole formation. In *Sources and detection of dark matter in the universe. Proceedings, 3rd International Symposium, and Workshop on Primordial Black Holes and Hawking Radiation, Marina del Rey, USA, February 17-20, 1998*, 1998.
- [48] M. Shibata and M. Sasaki. Black hole formation in the friedmann universe: Formulation and computation in numerical relativity. *Phys. Rev. D*, Vol. 60, p. 084002, Sep 1999.
- [49] J. Yokoyama. Cosmological constraints on primordial black holes produced in the near critical gravitational collapse. *Phys. Rev. D*, Vol. 58, p. 107502, 1998.
- [50] J. Yokoyama. Chaotic new inflation and formation of primordial black holes. *Phys. Rev. D*, Vol. 58, p. 083510, 1998.
- [51] R. Saito, J. Yokoyama, and R. Nagata. Single-field inflation, anomalous enhancement of superhorizon fluctuations, and non-Gaussianity in primordial black hole formation. *J. Cosmol. Astropart. Phys.*, Vol. 0806, p. 024, 2008.
- [52] C. T. Byrnes, E. J. Copeland, and A. M. Green. Primordial black holes as a tool for constraining non-Gaussianity. *Phys. Rev. D*, Vol. 86, p. 043512, 2012.
- [53] S. Young and C. T. Byrnes. Primordial black holes in non-Gaussian regimes. *JCAP*, Vol. 08, p. 052, 2013.
- [54] T. Nakama, T. Suyama, and J. Yokoyama. Supermassive black holes formed by direct collapse of inflationary perturbations. *Phys. Rev. D*, Vol. 94, No. 10, p. 103522, 2016.
- [55] T. Nakama, J. Silk, and M. Kamionkowski. Stochastic gravitational waves associated with the formation of primordial black holes. *Phys. Rev. D*, Vol. 95, No. 4, p. 043511, 2017.
- [56] T. Nakama, B. J. Carr, and J. Silk. Limits on primordial black holes from μ distortions in cosmic microwave background. *Phys. Rev. D*, Vol. 97, No. 4, p. 043525, 2018.
- [57] S. Dodelson. *Modern cosmology*. Academic Press, San Diego, CA, 2003.